The 2010 Pakistan Flood and the Russia Heat Wave:

Teleconnection of Extremes

William K. M. Lau[1], and K. M. Kim[2]

[1]Laboratory for Atmospheres, NASA Goddard Space Flight Center, Greenbelt MD, 20771

[2]Goddard Earth Sciences and Technology Center, U. of Maryland Baltimore County,

Baltimore Maryland, 21228

Submitted to Nature Geoscience

October 2010

Corresponding author: William K. M. Lau, Laboratory for Atmospheres, NASA Goddard Space Flight Center, Greenbelt, MD 20771. Email: William.K.Lau@nasa.gov. Tel: 301-614-6332

The Pakistan flood and the Russia heat wave/wild fires of the summer of 2010 were two of the most extreme events in the histories of the two countries occurring at about the same time. To a casual observer, the timing may just be a random coincidence of nature, because the two events were separated by long distances, and represented opposite forces of nature, *i.e.,* flood vs. drought, and water vs. fire. Here, we present evidences showing that the two events were indeed physically connected. Our results show that the root cause of the 2010 Russia heat wave/wild fires was an atmospheric blocking event in high latitudes which, through the excitation of a large-scale atmospheric Rossby wave, was instrumental in affecting the rainfall evolution of the South Asian summer monsoon, including triggering the development of a mid-tropospheric cyclone that was responsible for the torrential rain over Pakistan.

During July and August, 2010 Pakistan suffered the worst flood in 100 years. Over 1500 people and 1 million homes perished and 20 million were rendered homeless, or displaced from their homes by the floodwater. The total economic lost from property and crop damage, loss of businesses was in the tens of billions. At about the same time, Russia was stricken by a record heat wave, with temperature in Moscow rising above 40^{o} C for a prolonged period in July and August 2010, and the entire western Russia region (including western Siberia) was suffering from a prolonged drought. Intense and extensive wild fires raged over more than 5000 km^2 of forested area. The Russia heat wave, drought and forest fires might have taken over 5,000 lives and cost the economy loss more than 15 billion. By any measure, the Pakistan flood and the Russian heat wave /wild fires were super extreme events, both from the perspectives of

meteorology and society impacts. Already, the media, pundits and some scientists were wondering aloud whether the Pakistan flood and Russia heat wave and many of the extreme weather events experienced around the world in 2010 were the results of global warming. However, while the 2010 extreme events will likely add to the statistics of extreme events consistent with projections of global warming, no attribution can be made based on a single event. From past experience, an extreme event is seldom the result of a singular cause, but rather the end product of positive feedback from an alignment of multiple factors, on both large and small scales. In this study, we focus on such an alignment of factors leading to the Russian heat wave and the Pakistan flood. Our paper differs from previous studies of extremes in that we identify not only the causes of each event, but also the possible physical connection between them. Methodology and data used for this study are described in the Method Section at the end of the manuscript.

The Pakistan flood

Tucked away in the northwestern corner of the Indian subcontinent, and bounded on the northeast by the high mountains of Karakoram, on the west by the arid regions and deserts of Afghanistan, Syria and Iran, and on the south by the Arabian Sea, Pakistan is a relative dry region compared to monsoon India. Even during the peak of the monsoon season, July-August, the average total rainfall over the wettest part of the country (northern Pakistan) is of the order of 160-180 mm – a scanty amount compared to rain total of 1600-2000 mm for the same months over the wettest monsoon regions of northeastern India and the Bay of Bengal. Based on the NOAA Climate Prediction Center rainfall station data[1], during the 2 week period, July 25-August 8 2010, torrential rain of approximately 500 mm fell in about 10 days in the northern

Pakistan Swat Valley, exceeding more than 70% of the total *annual* mean rainfall over the same region. As shown in rainfall anomaly field in Fig. 1a, the heavy rain over northern Pakistan was not isolated geographically, but appeared to be connected to excessive monsoon rainfall over northern and northeastern India along the foothills of the Himalaya, and central and northeastern Arabian Sea. Reduced rainfall was found over most part of central and southern India, and the southern Bay of Bengal, and along the coast of Myanmar. The widespread rainfall anomaly suggested that the Pakistan heavy rain was a part of a major shift in the entire monsoon rainfall pattern, which normally has the heaviest rainfall over Bangladesh and Bay of Bengal in August.

The Russian heat wave

Russia is a vast country, covering northeastern Europe and Siberia, stretching from the Arctic Circle southward to Ukraine and Kazakhstan, southeastward to Mongolia and northeastern China. The dominant vegetation is tundra in the extreme northern regions around the Arctic Circle, tiaga (boreal forest) in northern and central Siberia, and temperate forest and steppe grassland in the south. In western Russian, climatologically July-August is the rainy season, with mean monthly rainfall of 75-85 mm. However, atmospheric blocking condition which slows or prevents the passage of rain storms, may develop and last for weeks, leading to dry conditions and wild forest fires[2-4] . During July-August 2010, a record heat wave and drought developed and prevailed over western Russia. Temperature in Moscow in August soared to a record daily high of 40^{o} C (about 10 degree above the climatological mean). Prior to 2010, the highest temperature record in Moscow was set at 36.8^{o} C in August, 1920. During the two-week period coinciding with the Pakistan flood, the heat wave expanded to cover

western Russia, western Siberia, and Eastern Europe (Fig. 1b). The extreme hot and dry weather spurred ferocious forest fires over the vast taiga regions of western Russia and Siberia, and Ukraine, as evidence in the density of the satellite fire counts. Also noteworthy is that temperature contrast, with much cooler temperature prevailed in the adjacent regions to the heat wave, over central and eastern Siberia, and western Europe.

Teleconnection

Figure 2 shows the time series of rainfall from TRMM over northern Pakistan [32-35N, 70-73E] and surface temperature from AIRS and fire count from MODIS over western Russia [45-65N, 30-60E]. Very heavy rain fell over northern Pakistan intermittently in clusters of 3-4 days during the two-week period from July 25- August 10, following a period of steadily increasing rainfall beginning in mid-June. Surface temperature over western Russia rose rapidly around June 20; remained at a high level for the next 10 days or so, and soared from around July 18 to reach a very high-level, with maximum area-averaged temperature exceeding nearly 9^{o} C above the seasonal mean, during a 2-week period contemporaneous with the heavy rain over Pakistan. The Russia forest fire activity, as evident from the MODIS fire count, was near normal or slightly elevated about the same time as the heat wave emerged, but dramatically intensified around July 25 and remained at a very high level till August 10, and dropped off rapidly, as a cold front passed through and brought rain to the area. The correlation between surface temperature and fire count is 0.70, and between fire count, surface temperature and Pakistan rainfall is 0.50 and 0.37, respectively. All correlations are statistically significant at the 95% level. The high correlation between heat wave and forest fire is expected, because the abnormally hot and dry air associated with the heat wave is conducive to forest fire. However,

the significant correlations of Russian surface temperature and forest fire count with Pakistan rainfall hint at a more profound teleconnection between the extratropics and tropics. In the following, we explore the physical basis for such a teleconnection. To facilitate the discussion of the evolution of the teleconnection pattern, we carry out separate but identical analyses for the 15-day period (Period II: July 25- August 8) for the Pakistan heavy rain, and for the 15-day antecedent period (Period I: June 10- 24).

Period I: July 10- July 24

This period characterized the development of the Russian heat wave and large-scale circulation and moisture conditions leading to, but *before* the Pakistan heavy rain. A pronounced blocking high, with 500 hPa geopotential height anomaly exceeding 120 -140 m was found over northern Europe and western Russia (Fig. 3a). The blocking high was coupled to a deep trough to its west, and another high pressure feature further east over western Siberia. The trough displayed a pronounced southwest-to-northeast tilt, penetrating into the subtropics with a cut-off low to the north of Pakistan. This pattern resembled that of a dispersive Rossby wave-train[6] emanating from the blocking high over western Russia, and propagating towards the east and southeast directions. As will be shown later, the penetrating trough and cut-off low (marked **L** in Fig. 3a) were associated subsequently with the formation of a mid-tropopsheric cyclone (MTC) which was responsible for the heavy rain over Pakistan. An MTC is a hybrid midlatitude-tropical, rain bearing weather system commonly found in the South Asian monsoon region[7-8].

Coupled to the 500 hPa blocking high was a lower troposphere large-scale anticyclone (Fig3b). The southerly flow on the west side of the anticyclone, brought warmer and moister

(rising) air to central and northern Europe, while the northerly flow on the eastern side brought widespread cooler (sinking) and drier air over western Siberia to regions further south. [See Fig. S1 in Supplementary Material for a description of the 500 hPa vertical motion pattern]. Over the mountainous region of Afghanistan and Pakistan, the low level flow was not well organized. However, over the larger South Asian monsoon region, two distinct branches of anomalous low- level flow could be identified. A strong low-level easterly flow from the Bay of Bengal was found over northern India. This flow opposed the climatological low level westerly monsoon flow, and implied an anomalous transport of moisture from the Bay of Bengal to northwestern India/northern Pakistan and the northern Arabian Sea. Additionally, an anomalous southerly low-level flow was found over northern Arabian Sea. Our analysis (figure omitted) showed that the northern Arabian Sea was warmer than normal at this time. The warmer Arabian Sea could increase evaporation, allowing more moisture transport by the anomalous southerlies into the Gulf of Oman and southern coast of Pakistan (Fig. 3b).

Period II: July 25 – Aug 7

During this period, the heat wave soared and the Russian wild fires grew in area coverage and intensity. At 500 hPa, the blocking high shifted about 20^{o} eastward in longitude, and grew to a very impressive size, with anomaly at the center exceeding 180 m (Fig. 3c). Examination of the daily variability of the 500 hPa geopotential height revealed that during the first week of this period, the slow eastward movement of the blocking high coupled with the rapid westward retrogression of the penetrating trough in the Rossby wave resulted in a separation of the cut-off low from the main trough. An explosive cyclogenesis of the low into a full-blown MTC west of northern Pakistan (marked C_1 in Fig. 3c) ensued. The strong mid-tropospheric ascent east of

157 the 500 hPa vortex - an evidence of the baroclinic structure of the MTC, was the reason for the
158 heavy rain over northern Pakistan [See Fig. S1b in Supplementary Material]. Notice that C_1 was
159 only a part of the large-scale anomalous circulation pattern of the entire South Asian monsoon
160 system, which included the development of a secondary MTC (marked C_2 in Fig. 3c) over
161 southern Pakistan and northeastern Arabia Sea, and an anomalous anticyclonic over western
162 China, northeast of the Tibetan Plateau.

163 In the lower troposphere, contemporaneous with the mid-tropospheric development, the
164 low level anticyclone over northern Europe and Russia shifted eastward to western Siberia (Fig.
165 3d). Strong southerly flow on the west of the anticyclone advected more warm and moist air
166 to northern Europe and the Arctic. On the southeastern side of the anticyclone, the low level
167 northeasterly, and northerly flow brought a tongue of dry and cold (sinking) air from Siberia to
168 Iran, and eastern Pakistan, setting the stage for a confrontation with the warm, moist (rising)
169 air from the north Arabian Sea to Pakistan, eventually leading to the MTC cyclogenesis.
170 Computations of the wind divergence (figures omitted) indicated that the MTCs were
171 associated with strong upper level wind divergence east of the mid-tropospheric low center.
172 The combination of strong mid-troposphere ascent and upper level divergence associated with
173 the MTCs would act like a pump drawing the low level southeasterly flow over northern India,
174 along the Indian/Nepal Himalayas, and transporting additional moisture from the Bay of Bengal
175 to Pakistan (Fig. 3d). The moist southeasterly flow along the Himalayas foothills could lead to
176 orographically forced heavy rain along the foothills region. The north and northwesterly flow
177 from an anomalous anticyclone over the southern tip of the India subcontinent could also have
178 contributed additional low-level moisture from the Arabian Sea, fueling the development of the

179 secondary MTC (C_2 in Fig. 3c). Overall, the large-scale circulation, the MTCs, and associated
180 large-scale vertical motion and upper wind divergence are dynamically consistent with the
181 rainfall anomaly over Pakistan, the Indian/Nepal Himalaya foothills, and the northeastern
182 Arabian Sea as shown in Fig. 1a.

183 J**etstream modulation**

184 During Period-I and –II, the strength of atmosphere blocking and the accompanying
185 Rossby wave were such that they distorted the flow of the powerful jetstream in the upper
186 troposphere, which in turn altered the steering of storm tracks. Climatologically, the boreal
187 subtropical jetstream comprises of a belt of fast moving westerly in the upper troposphere
188 around the global, centered around 35-40^{o}N, with compensating easterlies over the tropics.
189 Storms with mid-latitude origins are generally confined to the vicinity just south of the
190 jetstream maximum, and north of the zero-wind (zonal) line. During Period-I (figure omitted),
191 associated with the blocking development, there was a strengthening of the climatological
192 subtropical jetstream, and a new, weaker polar jetstream emerged over Scandinavia. During
193 Period-II, the Rossby wave influence on the jetstream was very pronounced. Here, the split
194 polar jetstream was displaced eastward from Period-I and found over northwestern Siberia and
195 the Arctic region of Eurasia (Fig. 4a). The subtropical branch, where the climatological westerly
196 belt was normally located (line contours in Fig. 4a), showed a highly wavy pattern spanning
197 southern Europe, the Mediterranean/North Africa, the Caspian Sea, Syria, northwestern China
198 and Mongolia, with the southernmost extent of the main jetstream hanging northwest of
199 Pakistan (Fig.4a). The signature of the Rossby wavetrain was even more pronounced in the 200
200 hPa meridional wind component (Fig.4b), showing a northern component around the Arctic

201 circle of Eurasia and a subtropical component from the Mediterranean to the western Pacific.
202 The magnitude of the subtropical branch was much stronger than climatology (line contours in
203 Fig. 4b), and the phase of the Rossby wave was almost in quadrature, with a westward phase
204 shift relative to that from climatology. The anomalous southerlies and the northerlies at 35-40^{o}
205 N west of Pakistan, indicated cyclonic circulation, consistent with the MTC formed over the
206 region. Given the planetary scale of the jetstream anomalies, it is conceivable that these
207 anomalies are connected to other major extreme weather events from Europe to Asia, in both
208 the tropics and extratropics during the summer of 2010.

209 **Conclusion and discussion**

210 We have presented preliminary evidences suggesting that the two record setting extreme
211 events in the summer of 2010*, i.e.,* the Russia heat wave/wild fires and the Pakistan flood are
212 meteorologically connected. The prolonged atmospheric blocking situation associated with the
213 extreme heat wave/drought and wild fires over western Russia is instrumental in forcing a
214 large-scale atmospheric Rossby wave train connecting western Russia to the South Asian
215 monsoon region. A deep trough in the Rossby wave penetrating from the mid-latitudes to the
216 tropics may have triggered the explosive cyclogenesis of a subtropical MTC, spawning the
217 extreme rainfall events over Pakistan, the Indian/Nepal Himalayas, and northeastern Arabian
218 Sea. The MTCs are known rain activators in the South Asian monsoon region, with both
219 midlatitude (baroclinic) and monsoonal (condensational heating) characteristics, including
220 warm core structure above 600 hPa, pronounced cyclonic structure in mid-troposphere, and
221 strong upper level divergence [7,9-10]. Further studies of the causes of the Pakistan flood should
222 revive the attention to the MTC as an important heavy rain-bearing monsoon weather system.

wlau 10/6/10 9:37 PM
Deleted: found

The present results raise important unanswered questions. For the South Asian monsoon region, rainfall is generally enhanced by La Nina*, i.e.*, below normal sea surface temperature (SST) in the eastern tropical Pacific, and above normal SST in the western Pacific and Indian Ocean. During the summer of 2010, a weak La Nina condition was brewing over the central eastern Pacific. Did the La Nina condition in 2010, including the warmer Arabian Sea, further add to the alignment of factors, favoring more rainfall over Pakistan? Could the Pakistan flood have occurred, if there were no Rossby wave forcing? Or with Rossby wave forcing but no pre-conditioning of the tropics, such as La Nina and warmer Arabian Sea? For the Russia heat wave and wild fires, the key question is : what caused the prolonged blocking situation that led to the unprecedented severity of the drought and west Russian forest fires? Previous studies showed that soil moisture and land surface processes played a vital role in the blocking event associated with severe summer heat waves, such as that occurred over Europe in 2003[11] . Are the 2010 and 2003 heat waves similar or different in terms of forcing and responses? The exceptional large amount of aerosols emitted from the 2010 Russia wild fires during Period-II (see Supplementary Material Fig. S2) would certainly have affected the surface and atmospheric energy budget over the west Russia and adjacent regions. Did aerosols from the forest fires play a role, via radiative heating and feedback processes in the atmosphere and at the surface, in amplifying and/or sustaining the atmospheric blocking? If so, this raises the intriguing possibility that the Russia wild fires may have contributed to the Pakistan flood! Finally, is this extraordinary teleconnection of extremes a sign of a changing atmospheric general circulation associated with global warming, favoring more extratropical-tropical

244 interaction? These are important and urgent questions that the scientific communities have to
245 provide answers, the sooner the better.

246 **Methods**

247 For this investigation, we used a combination of in-situ, satellite and reanalysis data to
248 carry out correlative and diagnostic analyses. Anomalies were defined as the deviations from
249 the climatology of each dataset. We used the satellite rainfall, fire count, and surface
250 temperature to examine the spatial patterns of the Pakistan heavy rain, and the Russian heat
251 wave and wild fires, and establish the temporal correlations among these variables. We then
252 defined two 15-day periods to identify the quasi-stationary features in the geopotential, wind
253 and moisture teleconnection patterns, prior to, and during the Russian heat wave and the
254 Pakistan flood. We seek physical and dynamical consistency among these independent data
255 with respect to evolving coherent spatial patterns during the two periods. For rainfall, we used
256 daily gridded rain gauge data from NOAA Climate Prediction Center (CPC)[1] , as well as daily
257 rainfall product (3B42) on 0.25 x 0.25 degree latitude-longitude grid from the Tropical Rainfall
258 Measuring Mission (TRMM)[5] . Surface temperature was estimated from the Advanced Infra
259 Red Sounder (AIRS), fire counts and aerosol optical thickness from the Moderate Resolution
260 Imaging Spectro-radiometer (MODIS) on board the NASA Aqua and Terra satellites. AIRS is a
261 high spectral resolution spectrometer on board Aqua satellite with 2378 bands in the thermal
262 infrared (3.7 - 15.4 μm) and 4 bands in the visible (0.4 - 1.0 μm). The MODIS Fire Pixel Count
263 has a spatial resolution of 1kmx1km and is determined by a significant increase in radiance at
264 4um compared to 11um radiance. It is available from the Terra and Aqua satellites twice daily,
265 night and day. Locations of fire pixel from all four daily measurements are used in Fig. 1 and

Fig. 2. Data and meta-data for AIRS and MODIS fire count were obtained from at the Goddard Earth Sciences Data and Information Service Center (http://disc.sci.gsfc.nasa.gov/AIRS) and MODIS Hotspots/Active Fires Text file FTP site (ftp://mapsftp.geog.umd.edu), respectively. For geopotential height, wind, and moisture, we used the National Center for Environmental Prediction (NCEP) reanalysis data available from (http://ftp.cdc.noaa.gov).

271

272 **References**

273 1. Xie, P et al., A gauge-based analysis of daily precipitation over East Asia, *J.*
274 *Hydrometeorol*. **8** 607-626 (2007)

275 2. Ogi, M., Yamazaki, K. and Tachibana, Y. The summer northern annual mode and
276 abnormal summer weather in 2003. *Geophys. Res. Lett*. **32**, L04706,
277 doi:10.1029/2004GL021528 (2005)

278 3. Groisman, P.Y., Sherstyukov, B.G., Razuvaev, V.N. et al., Potential forest fire danger over
279 Northern Eurasia: changes during the 20th century. *Global and Planetary Change* **56**,371–
280 386 (2007)

281 4. Girardin, M. P.et al., Heterogeneous response of circumboreal wildfire risk to climate
282 change since the early 1900s. *Global Change Biology* **15**, 2751–2769, doi: 10.1111/j.1365-
283 2486.2009.01869.x (2009)

284 5. Huffman, G. J. et al., The TRMM Multisatellite Precipitation Analysis (TMPA): Quasi-
285 Global, Multiyear, Combined-Sensor Precipitation Estimates at Fine Scales. *J. Hydrometeor.*
286 **8**, 38–55 (2007)

287 6. Hoskins, B. J. and Ambrizzi, T. Rossby Wave Propagation on a Realistic Longitudinally
288 Varying Flow. *J. Atmos. Sci.* **50**, 1661-1671 (1993)

289 7. Krishnamurti, T. N. and Hwakins, R. S. Mid-Tropospheric Cyclones of the Southwest
290 Monsoon. *J. Appl. Meteor*. **9**, 442-458 (1970)

291 8. Carr, F. H. Mid-tropospheric cyclones of the summer monsoon. *Pure Appl. Geophys*. **115**,
292 1383-1412 (1977)

9. Mak, M. K. The Monsoonal Mid-Tropospheric Cyclogenesis. *J. Atmos. Sci.* **32**, 2246-2253 (1975)

10. Goswami, B. N., Keshavamurty, R. N. and Satyan V. Role of barotropic, baroclinic and combined barotropic-baroclinic instability for the growth of monsoon depressions and mid-tropospheric cyclones. *J. Earth Sys. Sci.* **89**, 79-97 (1980)

11. Ferranti, L. and Viterbo, P. The European Summer of 2003: Sensitivity to Soil Water Initial Conditions. *J. Climate* **19**, 3659–3680 (2006).

Acknowledgements

This work was supported by the NASA Interdisciplinary Investigation, and the Tropical Rainfall Measuring Mission (TRMM).

Author contributions

W.K.M.L. led the study and wrote the manuscript. K.M.K. carried out the data analyses. Both authors collaborated in the discussion of the results and writing.

Additional information

The authors declare no competing financial interests.

Figure Captions

Figure 1 Spatial distribution of a) TRMM rainfall anomaly over Pakistan and the South Asian monsoon region for period July 25 – Aug 8, 2010, b) AIRS surface temperature anomaly, and MODIS daily fire count (green dots) for the same period. The rainfall anomaly (mm day^{-1}) was derived from the base period of 1988-2009, and the surface temperature anomaly (^{o}C) from the base period of 2003-2009.

Figure 2 Time series of AIRS daily surface temperature (^{o}C) averaged western Russia [45-65^{o} N, 30-60^{o}E], with positive (negative) deviations from climatology shaded red (blue), MODIS fire count per day (right ordinate) over the same domain, and TRMM daily rainfall (mm day^{-1}, left ordinate) over northern Pakistan [32-35^{o}N, 70-73^{o}E], for the June 1 - August 27, 2010.

Figure 3 Spatial patterns of a) 500 hPa geopotential height and wind anomalies during Period-I, b) 850 hPa wind and moisture anomalies during Period-I, c) 500 hPa geopotential height and wind anomalies during Period-II, and d) 850 hPa wind and moisture anomalies during Period-II. The geopotential height (m) and wind (ms^{-1}) data were from the NOAA National Center for Environmental Predication (NCEP). Centers of the blocking high (H), and low (L) and the mid-tropospheri c cyclones (C_1 and C_2) are marked. Anomalies were computed based on the climatology of 1979–2009.

Figure 4 Spatial pattern of a) 200 hPa zonal wind anomaly and climatology (shown in green line contours) showing the influence of Rossby waves on the jetstream flow, b) 200hPa meridional wind anomaly and climatology (shown in green line contours), showing the

Rossby wave signature at the jetstream level. Anomalies were computed based on the climatology of 1979-2009.

336

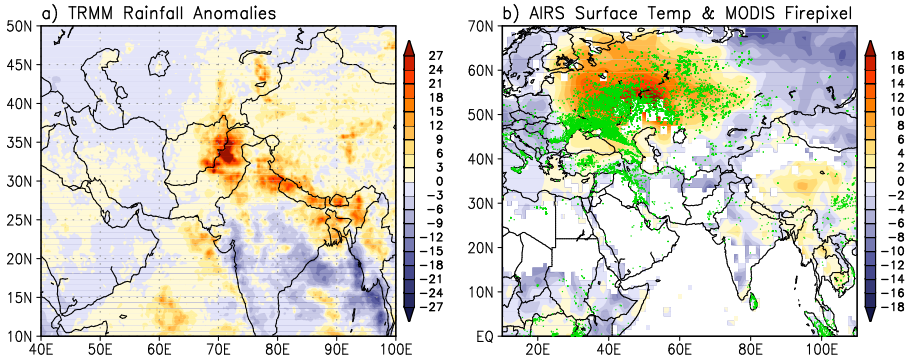

337

338 Figure 1

339

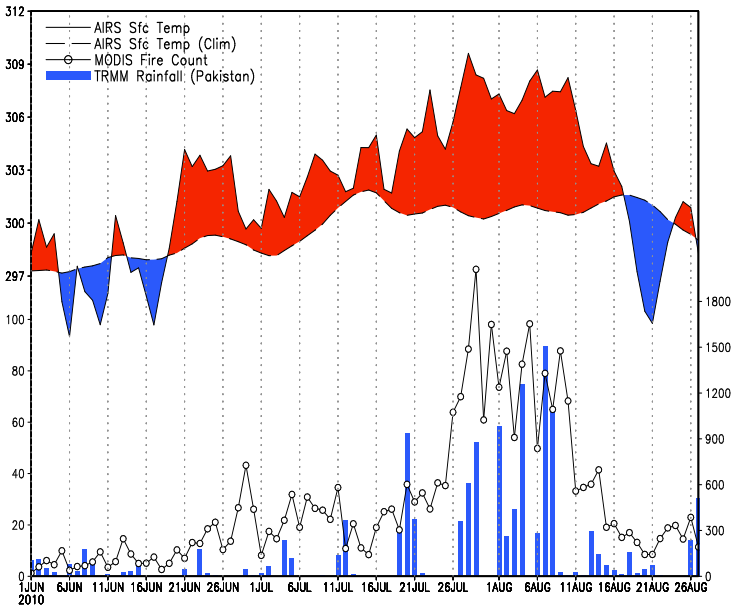
AIRS Sfc Temp
AIRS Sfc Temp (Clim)
MODIS Fire Count
TRMM Rainfall (Pakistan)
312
309
306
303
300
297
100
80
60
40
20
0
1800
1500
1200
900
600
300
0
1JUN
2010
6JUN
11JUN
16JUN
21JUN
26JUN
1JUL
6JUL
11JUL
16JUL
21JUL
26JUL
1AUG
6AUG
11AUG
16AUG
21AUG
26AUG

Figure 2

342

343

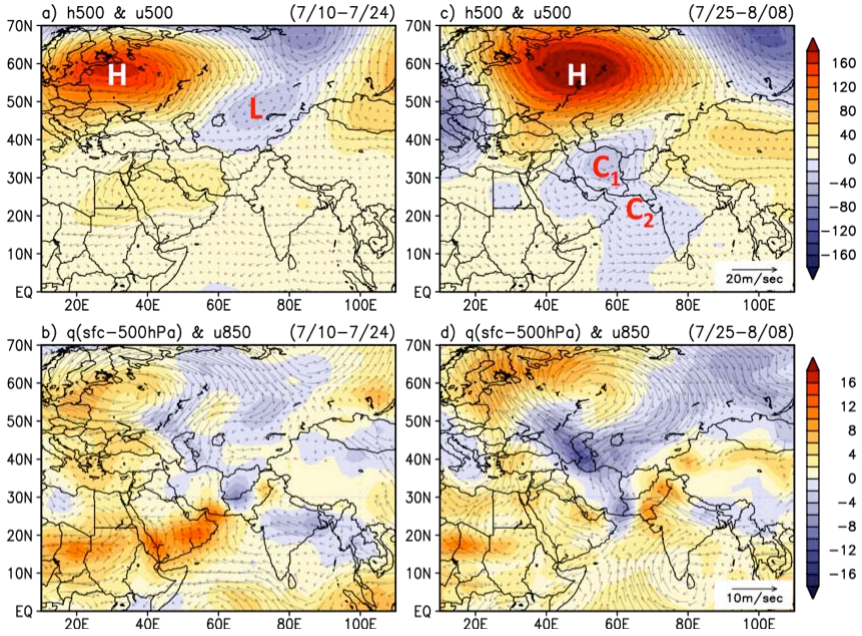

344

345 Figure 3

346

346

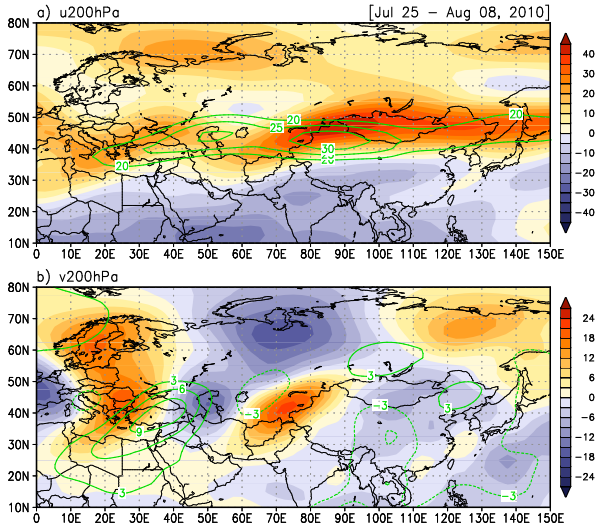

347

348 Figure 4

Supplementary Material

Mid-tropospheric vertical motion

During Period-I, wide-spread large-scale sinking motion (negative anomaly) was found east of, and rising motion (positive anomaly) west and southwest of the blocking high (H) (Fig. S1a). The vertical motion pattern was consistent with the anticyclonic flow associated with the blocking, having subsiding colder air moving toward the subtropics and poleward moving warmer air towards western Europe. Strong sinking motion was also noted over western Afghanistan and Iran, probably associated with a large-scale anomalous anticyclone found over Saudi Arabia and Iran (see Fig. 3a). With respect to the mid-tropospheric low (L), rising motion was found to its southeast, and sinking motion to its northwest, typical of the baroclinic structure of a developing low in mid-latitudes. In the tropics, rising motion was found over northern Pakistan, northern India, and the northern Arabian Sea, coupled to sinking motion over the Bay of Bengal, and Indo-China. The rising motion, though still moderate in magnitude provided vertical transport of moisture to the lower and middle troposphere, ready to be tapped for MTC development. During Period-II (Fig. S1b), the subsiding (colder) air over western Siberia east of the blocking high (H) became more expansive and amplified, with the southern tip of the sinking air reaching below 30N over Iran. At the same time, eastern and northern Europe experienced generally rising motion as the block shifted eastward. In the subtropics and tropics, the MTCs (C_1 and C_2) were fully developed over Iran/Afghanistan, and the northern Arabia Sea. Clearly from the vertical motion field, strong upward motion coinciding with the Pakistan flood was found to the east, and sinking motion to the west of the primary MTC (C_1), which was the primary weather system that caused the heavy rain over

371 northern Pakistan. For C_2, the rising motion was more coincident with the vortex center, more
372 representative of a monsoon weather system. It should be pointed out that the vertical
373 motion fields were derived from rather coarse resolution (2.5^o x 2.5^o latitude-longitude) wind
374 analyses, and therefore reflected only the large-scale vertical motion pertaining to the synoptic
375 scale forcing associated with the blocking in high latitudes and the rainfall in the monsoon
376 region. The convective scale vertical motions directly associated with updrafts in the heavy rain
377 were not resolved in the analysis.
378
379 **Aerosol distribution**
380 The 2010 Russia wild fires emitted abundant smoke, noxious gases (CO_2, CO, CH_4, NOx,
381 and others) and aerosols (black carbon and organic carbon) harmful to human health, and
382 possibly alter the land surface and atmospheric heat balance, depending on the radiative
383 properties of the gases and aerosols. These gases and aerosols were transported by the
384 atmospheric circulation to high elevations and regions far from the forest fire. During Period-I
385 (July 10-24), atmospheric loading of aerosols over Russia and Siberia was actually slightly below
386 normal over vast regions of Eurasia and the Asian monsoon region (Fig. S2a). During Period-II
387 (July 25- August 8), as the heat wave soared and the forest fire raged, the aerosol loading in the
388 atmosphere increased dramatically (Fig. S2b). Maximum high level of aerosol concentration
389 (AOD>1) was found over a large region, near but slightly offset to the west of the center of
390 surface anticyclone, and downwind of the region of maximum fire count (See Fig. 1b in main
391 text). High-to-moderate aerosol concentrations (AOD>0.5) were found over northwestern
392 Europe, the Arctic circle, regions north of the Caspian Sea, western Russia in conjunction of

393 the slow eastward migration, and growth in size and magnitude of the blocking event. Large
394 negative AOD (<0.6-0.8) anomaly was found over Pakistan, northwest India and the Indo-
395 Gangetic Plain. This was associated with the wash-out, by the excessive rain, of the dense
396 aerosol (mostly dust and black carbon) which accumulate in the region during the early
397 monsoon season[1,2]. The strong contrast between the large areas of high aerosol loading over
398 western Russia, and the overall reduced aerosol loading over the pan-continental regions of
399 Eurasian, Mediterranean, Africa and monsoon Asia would most likely have affected the
400 energy balance through the direct and semi-direct effects[3], and thus could play a role in
401 sustaining and/or amplifying the Russian heat wave, the blocking high and indirectly the
402 Pakistan flood, through the Rossby wave teleconnection.
403

References for Supplementary Material

1. Lau, K. M., Kim, M. K., and Kim, K. M., Aerosol induced anomalies in the Asian summer monsoon: The role of the Tibetan Plateau. *Climate Dynamics* **26** (7-8), 855-864, doi:10.1007/s00382-006-0114-z (2006).

2. Gautam, R., Hsu, C., and Lau, K. M., Pre-monsoon characterization and radiative effects over the Indo-Gangetic Plain: Implications for regional climate warming. *J. Geophys. Res*. **115**, D17208, doi:10.1029/2010JD0 (2010).

3. Hansen, J., Sato, M. and Ruedy, R. Radiative forcing and climate response. *J. Geophys. Res.* **102**, 6831-6864 (1997)

wlau 10/6/10 9:40 PM
Formatted: List Paragraph, Indent: Left: 0", Hanging: 0.31", Line spacing: double, Numbered + Level: 1 + Numbering Style: 1, 2, 3, ... + Start at: 1 + Alignment: Left + Aligned at: 0.44" + Indent at: 0.69", Tabs:

wlau 10/6/10 9:40 PM
Deleted:
<#>

wlau 10/6/10 9:40 PM
Formatted: Font:12 pt

3.

Figure Caption for Supplementary Material

Figure S1. Spatial pattern of vertical motion at 500 hPa for a) Period-I and b) Period-II. Ascending (descending) motion is shaded red (blue). Labels denote position of low centers at 500 hPa. Sign of the vertical motion is reversed, and the unit is Pa s^{-1} The centers of the 500 hPA blocking high (H) and low (L), and the MTC's (C_1 and C_2) are marked to show their relative positions with respect to the vertical motion field.

Figure S2 Spatial patterns of a) MODIS Aerosol Optical Depth (AOD) and 850 hPa wind anomalies (ms^{-1}) during Period-I, and b) Same as in a), but for Period- II.

Figure S1

wlau 10/6/10 9:40 PM
Deleted:

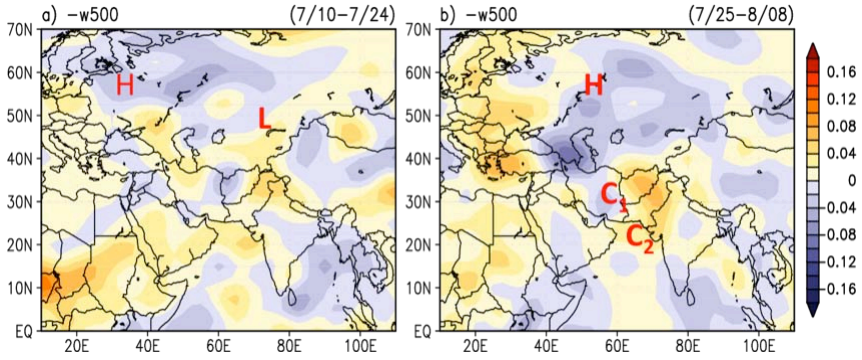

427

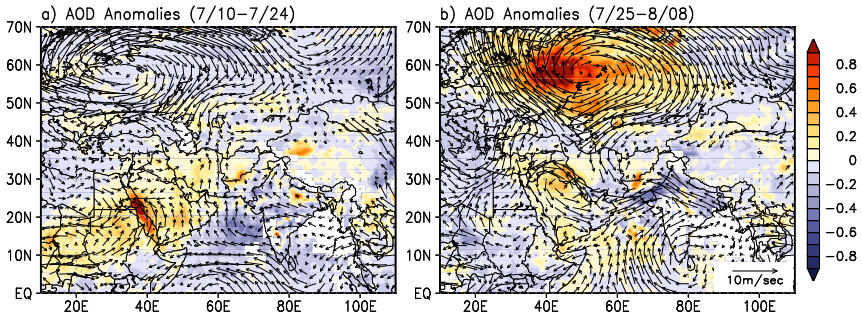

428

429 Figure S2

430